npj | biofilms and microbiomes

Article

Published in partnership with Nanyang Technological University

https://doi.org/10.1038/s41522-024-00586-6

A phosphate starvation induced small RNA promotes *Bacillus* biofilm formation

Yulong Li[1,2,6], Xianming Cao[1,6], Yunrong Chai[3], Ruofu Chen[1], Yinjuan Zhao[1], Rainer Borriss[4], Xiaolei Ding[1], Xiaoqin Wu[1], Jianren Ye[1], Dejun Hao[1] ✉, Jian He[5], Guibin Wang[1], Mingmin Cao[1], Chunliang Jiang[1], Zhengmin Han[1] & Ben Fan[1] ✉

Currently, almost all known regulators involved in bacterial phosphorus metabolism are proteins. In this study, we identified a conserved new small regulatory RNA (sRNA), named PhoS, encoded in the 3' untranslated region (UTR) of the *phoPR* genes in *Bacillus velezensis* and *B. subtilis*. Expression of *phoS* is strongly induced upon phosphorus scarcity and stimulated by the transcription factor PhoP. Conversely, PhoS positively regulates PhoP translation by binding to the ribosome binding site (RBS) of *phoP* mRNA. PhoS can promote *Bacillus* biofilm formation through, at least in part, enhancing the expression of the matrix-related genes, such as the *eps* genes and the *tapA-sipW-tasA* operon. The positive regulation of *phoP* expression by PhoS contributes to the promoting effect of PhoS on biofilm formation. sRNAs regulating biofilm formation have rarely been reported in gram-positive *Bacillus* species. Here we highlight the significance of sRNAs involved in two important biological processes: phosphate metabolism and biofilm formation.

Phosphorus (P) is the fifth most abundant element (after C, H, O, and N) on earth and is essential for the growth of all organisms, including microbes. In the natural environment, microorganisms often encounter inorganic phosphorus (Pi) limitation[1], which has driven the development of a dynamic system enabling them to sense and respond to this critical environmental (extracellular) signal. The regulatory systems that bacteria use for control of the phosphate (Pho) regulon, that is, the PhoR-PhoB system in gram-negative bacteria such as *Escherichia coli* and the PhoP-PhoR system in gram-positive bacteria such as *Bacillus subtilis*[2], serve as a paradigm for studies of the so-called two-component system (TCS). In both systems, the first protein is a sensory histidine kinase with an integral membrane domain, and the second is a cognate response regulator and a transcription factor. Understanding the regulatory network in phosphate metabolism is important not only for applications of microorganisms in agriculture, such as the development of biocontrol agents and microbial fertilizers, but also for pharmaceutical and industrial production. For instance, in fermentation tanks, high phosphate levels often result in a low yield of desired secondary metabolites[3], while reduced phosphorus levels usually lead to a significant decrease in microbial growth. The paradox may be addressed when people have a comprehensive understanding of the regulation mechanisms governing phosphate metabolism in bacteria. In bacteria, proteins have been identified as the dominant regulators of phosphate metabolism thus far, with few reports on the involvement of other types of regulators, such as sRNAs[4]. This knowledge gap presents an intriguing opportunity for exploration.

Biofilms, which are highly structured aggregates formed by microorganisms at two-phase interfaces, are the prevalent form of bacterial communities in nature[5]. Bacterial cells in biofilms are encased in a self-produced extracellular matrix, which in the case of the model microorganism *B. subtilis* contains two major substances: an exopolysaccharide (EPS) and the fibrous protein TasA[6,7]. EPS is synthesized by the products of a 15-gene *epsABCDEFGHIJKLMNO* operon (hereafter referred to as the *eps* operon), while TasA is a type of protein forming a fiber scaffold[7] produced and assembled by the *tapA-sipW-tasA* operon[8–10]. Biofilm formation has been widely studied due to its clinical and industrial relevance, and in-depth insights into its underlying regulatory mechanisms have been obtained. Among the regulatory factors that control biofilm formation, most are proteins, although there are also sRNAs found to be involved, mostly in gram-negative bacteria such as *E. coli* and *Salmonella typhimurium*[11–18]. In a few reports, sRNAs are also linked with biofilms in gram-positive bacterial pathogens such as *Staphylococcus aureus*[19,20]; however, little has been revealed on how sRNA governs biofilm formation in gram-positive beneficial species such as *B. velezensis* and *B. subtilis*.

[1]Co-Innovation Center for Sustainable Forestry in Southern China, College of Forestry and Grassland, Nanjing Forestry University, Nanjing, China. [2]School of Agriculture, Ningxia University, Ningxia, China. [3]Department of Biology, Northeastern University, Boston, USA. [4]Institut für Biologie, Humboldt Universität Berlin, Berlin, Germany. [5]College of Life Science, Nanjing Agricultural University, Nanjing, China. [6]These authors contributed equally: Yulong Li, Xianming Cao.
✉e-mail: djhao@njfu.edu.cn; fanben2000@gmail.com

The plant beneficial *B. velezensis* strain FZB42, phylogenetically close to *B. subtilis*[21], is the prototype of the group of gram-positive plant growth-promoting rhizobacteria (PGPR), which are of immense agricultural importance. FZB42 can form robust biofilms and produce more than 10 antibiotics that inhibit a diverse array of phytopathogens. As a model PGPR, FZB42 has been extensively studied in plant-microbe interactions. In a previous work, we identified dozens of sRNA candidates in FZB42 that may be involved in plant-microbe interactions[22]. In this work, we conducted an in-depth investigation on one of them, named PhoS. We found that PhoS is simultaneously involved in phosphorous metabolism and biofilm formation. We elucidated the molecular mechanisms underpinning these effects and their interlinking factors.

Results

PhoS is a 66-nt sRNA encoded in the 3'UTR of *phoR*

In a previous study, we detected a putative sRNA encoded in the intergenic region (IGR) between *polA* and *phoR* in *B. velezensis* FZB42[22]. The sRNA was named Bas01 and showed very abundant expression (Supplementary Fig. 1), at least compared to other sRNAs detected in the same study[22]. The deletion mutant of the Bas01 gene showed no significant difference in growth from the wild-type (Supplementary Fig. 2a); however, the total protein profile of the mutant differed noticeably from that of the wild-type for samples collected at three different time points during stationary phase (Supplementary Fig. 2b). In many reported cases, the effects of sRNAs on protein expression are subtle and barely observed in SDS-PAGE. Therefore, the results suggested that Bas01 may have a strong impact on FZB42 physiology. Given its location downstream of *phoR* and its function in phosphate response (as demonstrated below), we renamed Bas01 PhoS and used the name hereafter.

PhoS accumulates when cells enter the stationary phase in each of the four different media that we tested (8 and 10 h, Fig. 1a). Our dRNA-seq data showed that PhoS possesses a primary 5' end mapped to the 3'UTR of *phoR*, which was detected after terminator exonuclease (TEX) treatment of the RNA samples (Fig. 1b). We further confirmed the 5' end of PhoS by primer extension (Fig. 1c). A typical Rho-independent terminator was predicted at the 3' end of PhoS (Fig. 1d). The size of PhoS was determined to be 66 nt, consistent with the Northern blot result (Supplementary Fig. 1).

To confirm that *phoS* has its own promoter in the 3'UTR of *phoR*, we fused two DNA sequences of different lengths (~180 and ~360 bp) upstream of the *phoS* transcription start site to a promoter-less *gfp* and introduced the fusions to the *amyE* locus of FZB42. The observation of bright fluorescence of the reporter strains indicated that the region upstream of *phoS* contains its own promoter (Fig. 1e).

Sequence alignment revealed that *phoS* is highly conserved in different *Bacillus* species, including *B. subtilis* (Fig. 1f). There is also a highly conserved extended −10 motif in its promoter region. More strikingly, the sequence alignment also revealed a putative 'seed' region (a 17-nt C-rich motif) at its 5′ end, which is 100% conserved in all the *Bacillus* strains analyzed, indicating that PhoS may have a conserved function in *Bacillus*.

PhoS promotes biofilm formation in *Bacillus*

To determine functional roles of PhoS, we first performed studies using the *B. subtilis* DK1042 strain. *B. subtilis* is phylogenetically close to *B. velezensis*, both belonging to the same *B. subtilis* species complex. However, in contrast to the extreme difficulty in introducing a plasmid into *B. velezensis* FZB42, *B. subtilis* DK1042 demonstrates a high amenability to plasmid transformation[23], which allows us to overexpress *phoS* from a plasmid. We constitutively expressed the *phoS* gene in DK1042 by cloning it under the P_{spac} promoter in a self-replicable vector pDG148-stu[24] lacking an active *lacI* gene. The plasmid was introduced to DK1042 for phenotypic examination. We observed that colonies of DK1042 with *phoS* overexpression displayed more wrinkles than those carrying an "empty vector" (pDG148-stu carrying the terminator sequence of *phoS*) or no plasmid on LB agar (Fig. 2a, the first row). To confirm this phenomenon, we similarly cloned the *phoS* into pDG148-stu and introduced the resulting plasmid into *B. subtilis* 168 for observation. Similar to the result in DK1042, the 168 colonies carrying the *phoS* gene demonstrated a rougher surface on both LB agar (Fig. 2a, 2nd row) and MSgg agar (Fig. 2a, 3rd row). Based on these results, we inferred that PhoS overexpression may promote biofilm formation in *Bacillus*.

To test this inference in *B. velezensis* FZB42, we used its Δ*phoS* mutant since we could not introduce the *phoS*-overexpressing plasmid into it. While no visual difference was observed in pellicles between the wild-type and the deletion strain grown in regular LBGM broth (Fig. 2b, 1st row), when Congo Red was added to the medium, pellicles formed by the Δ*phoS* mutant appeared lighter than those formed by either the wild-type or the complementary strain (Fig. 2b, 2nd row). On LBGM agar plates with Congo red, colonies of Δ*phoS* also appeared lighter (Fig. 2b, 3rd row). The material stained by the dye was extracted and quantitatively assayed. The results showed that there was a reduced incorporation of Congo red in the pellicles of the Δ*phoS* mutant (Supplementary Fig. 3). Congo red has been used in staining biofilm because it strongly binds TasA, a kind of fibrous protein that is a main component of the biofilm matrix in *B. subtilis*[7,10]. These results suggest that PhoS might positively regulate TasA production.

We also made assays under other conditions using different media, different temperatures, and different strains (*B. velezensis* FZB42 and *B. subtilis* and DK1042). Similar effects of *phoS* on biofilm formation were obtained (Fig. 2c–e) (Supplementary Table 4). With all the results, we concluded that *phoS* could somehow promote biofilm formation of *Bacillus* species.

PhoS enhances expression of genes involved in *Bacillus* biofilm formation

To understand how PhoS promotes biofilm formation, we conducted transcriptome analysis of wild-type FZB42 and the Δ*phoS* mutant grown in RNB medium, a modified version of LB with reduced nutrients to promote earlier and stronger expression of PhoS. A total of 261 genes were identified to be differentially expressed in the Δ*phoS* mutant ($p < 0.05$), all of which had a fold change greater than three (Fig. 3a and Supplementary Table 1). The *tapA-sipW-tasA* operon genes were among the top downregulated genes in the Δ*phoS* mutant, consistent with the color differences observed above in colony morphology. Fourteen genes in the *eps* operon, together with *bslA*, a gene encoding hydrophobin for the water-repellent surface layer of biofilms[25], were also downregulated in the Δ*phoS* mutant. We selected some representative differentially expressed genes (DEGs), mostly known to be involved in biofilm formation, for independent qPCR validation (Fig. 3b, c). The results showed that they had decreased expression in the Δ*phoS* mutant compared to the wild-type (Fig. 3b) but increased expression in the *phoS* overexpression strain compared to DK1042 carrying an empty vector (Fig. 3c), consistent with the transcriptome data. Based on these findings, we propose that PhoS promotes biofilm formation in *Bacillus* by regulating these biofilm-related genes.

To further explore the relationship between *phoS*, the *tapA-sipW-tasA* operon, and the *eps* genes and their impact on the biofilm phenotype, we constructed double mutants in FZB42 and examined their biofilm phenotypes (Fig. 3d). The edge of the Δ*tasA* colonies was less wrinkled than that of the wild-type colonies (Fig. 3d), suggesting that TasA is responsible for the wrinkles in this region. Meanwhile, the Δ*epsA* mutant lacked aerial projections in the center of its colony surface compared to the FZB42 wild-type, indicating that the exopolysaccharides synthesized by the *eps* genes are mainly responsible for the projection structures in *B. velezensis* FZB42. This finding is consistent with a previous report on *B. subtilis*[8].

The Δ*tasA* mutant still exhibited aerial projections due to the presence of the *eps* genes (Fig. 3d); however, when *phoS* was further deleted (Δ*tasA*Δ*phoS*), the center of the colony became similarly smooth as the edge, indicating that *phoS* also promoted the EPS production. This is consistent with the transcriptome and qPCR results. Compared to the single Δ*epsA* mutant, the Δ*epsA*Δ*phoS* double deletion mutant showed reduced wrinkles in the edge region, which supported the inference that PhoS promotes *tasA*

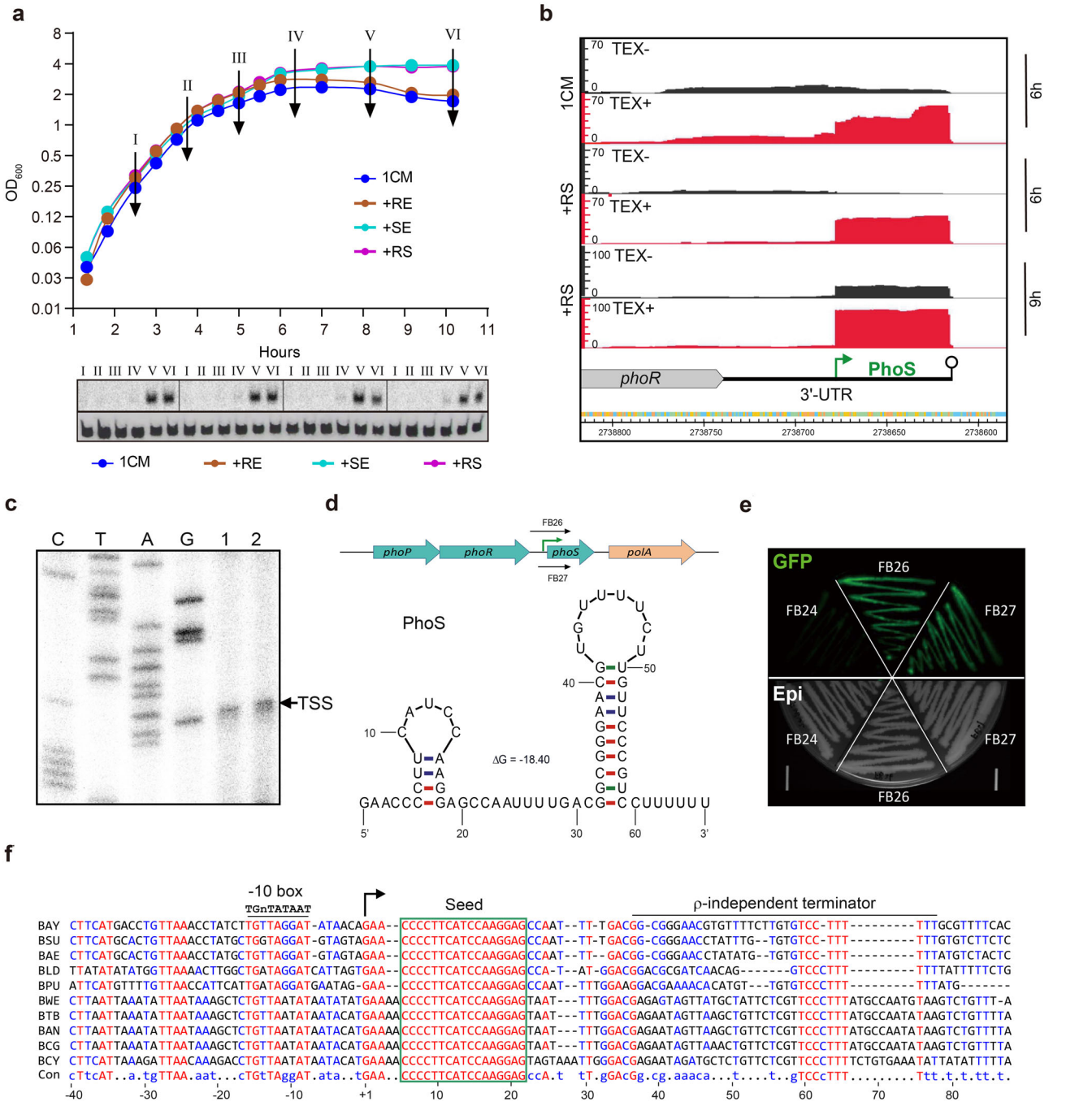

Fig. 1 | Expression and characterization of the sRNA PhoS in *B. velezensis* FZB42. **a** Expression profile of PhoS detected by Northern blot in four different media (1 CM, +RE, +SE, and +RS)[22]. Bacterial cultures were sampled for total RNA extraction at six different time points indicated by the arrows on the growth curves. The transcript of PhoS was determined by dRNA-seq sequencing reads (**b**) and primer extension (**c**). Lanes 1 and 2 in Panel C were identical sample loads; the transcription start site (TSS) of *phoS* is indicated by the arrow. **d** Gene arrangement of *phoS* (top) and secondary structure of PhoS (bottom) predicted by UNAfold[54]. **e** Analysis of the *phoS* promoter region of different lengths using GFP reporter constructs in three FZB42 derivatives, FB24 (*amyE*::promoterless-*gfp*), FB26 [*amyE*::$P_{phoS(\sim360bp)}$-*gfp*), and FB27 [*amyE*::$P_{phoS(\sim180bp)}$-*gfp*], visualized by UV (upper, GFP) and white light (bottom, Epi). **f** Sequence alignment of the *phoS* coding and flanking regions among related *Bacillus* species. BAY: *B. amyloliquefaciens* FZB42; BSU: *B. subtilis* subsp. subtilis 168; BLD: *B. licheniformis* DSM13; BPU: *B. pumilus* SAFR-032; BAE: *B. atrophaeus* BATR1942_12330; BWE: *B. weihenstephanensis* BcerKBAB4; BTB: *B. thuringiensis* BMB171; BCG: *B. cereus* G9842; BAN: *B. anthracis* Ames; BCY: *B. cytotoxicus* NVH 391-98. The +1 site of *phoS* in FZB424 is denoted by an arrow. Putative promoter motifs and Rho-independent terminator sequences are indicated.

expression, as suggested by the transcriptome data and the Congo red results (Fig. 2b). Notably, the Δ*tasA* colonies were also stained red, indicating that Congo red is not specific to TasA. We assume that EPS, in addition to TasA, can also bind to Congo red, considering its common use in staining other polysaccharides.

We conducted additional experiments to examine the impact of PhoS on the production of EPS in FZB42 and DK1042. Our findings revealed that disrupting *phoS* in FZB42 led to a significant decrease in EPS production, whereas constitutive expression of *phoS* in DK1042 and 168 apparently increased EPS production (Fig. 3e). This observation provides further

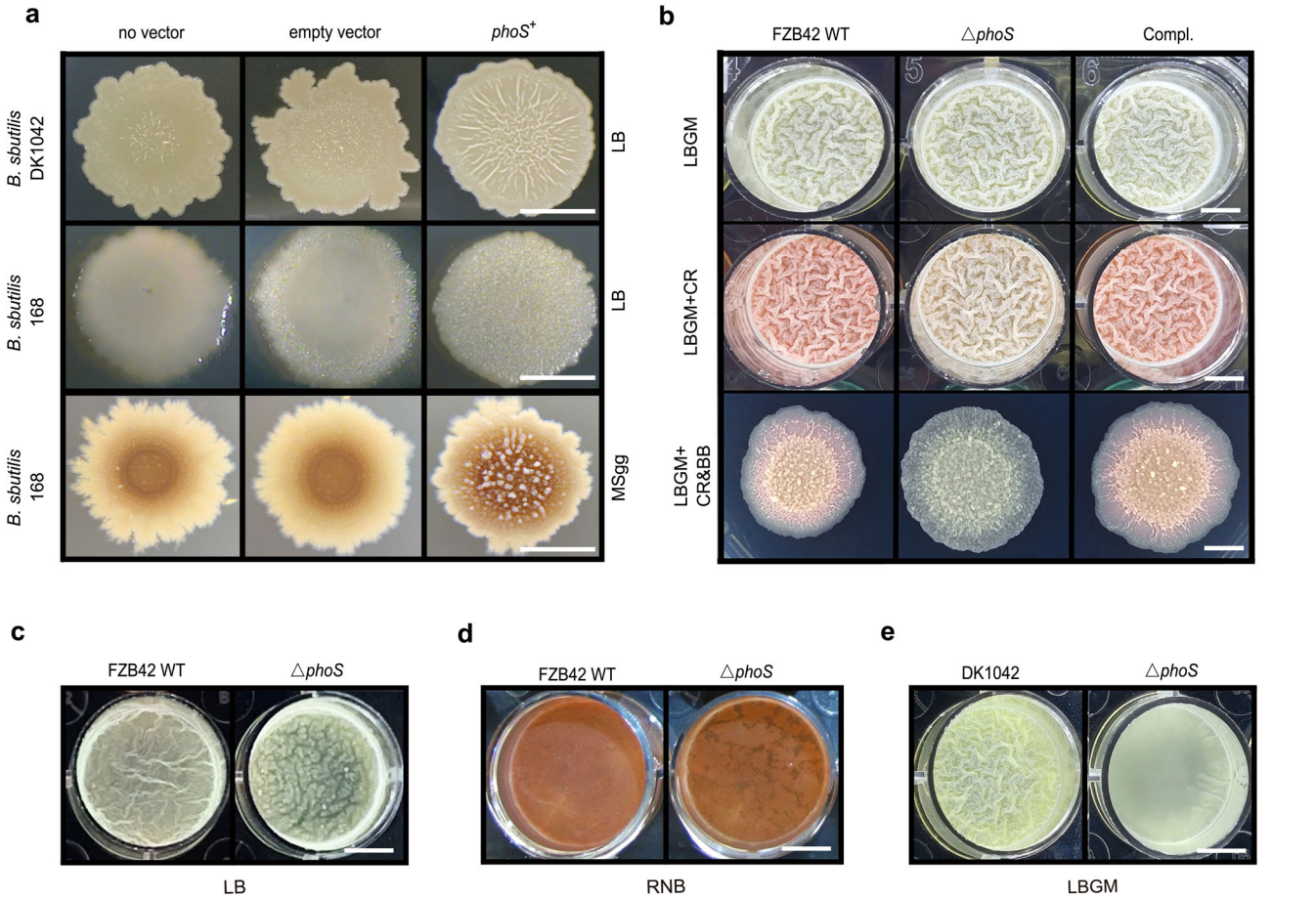

Fig. 2 | PhoS promotes biofilm formation in *Bacillus* species. a Effect of *phoS* on colony morphology of *B. subtilis*. *B. subtilis* 168 and DK1042 containing an empty vector (pDG148-stu), the vector carrying *phoS* (pDG148-stu/*phoS*+), or no vector were grown on LB agar plates (the first two rows) and MSgg agar plates (the 3rd row) at 25 °C for one week. Note that the colonies with overexpressing *phoS* (*phoS*+) had a rougher surface. **b** Effect of *phoS* deletion on biofilm formation in *B. velezensis* FZB42, whose wild type, Δ*phoS* mutant, and *phoS* complementation strain (Compl.) were grown in LBGM medium and LBGM with CR or on LBGM agar containing CR and Coomassie Brilliant Blue (BB). In (**a**, **b**), kanamycin was added to the media for the cells carrying a plasmid but not for the cells carrying no plasmid to maintain the plasmids. **c**–**e** Effect of *phoS* deletion on biofilm formation in (**c**, **d**) *B. velezensis* FZB42 and (**e**) *B. subtilis* DK1042, whose wild-type and respective Δ*phoS* mutants were grown in LB medium (**c**), RNB medium with CR (**d**), and LBGM medium (**e**). For each panel, one representative plate from three replicates is shown. In (**b**–**e**), the bacteria were grown in LBGM at 25 °C for 32 h (**b**, **e**), in LB for 10 h (**c**), in RNB medium containing CR for 72 h (**d**), and on agar plates for one week (**b**, 3rd row). Scale bar, 0.5 cm.

evidence for the role of PhoS in *eps* expression. Taken together, we conclude that PhoS promotes biofilm formation in FZB42 at least partially by positively regulating EPS and TasA-related matrix genes, although we demonstrated later that they are not direct targets of PhoS (see the discussion part).

Expression of *phoS* is induced by phosphate starvation and requires PhoP

Having unraveled that PhoS has a role in biofilm formation, we are equally intrigued by the mechanisms governing the regulation of PhoS. The proximity of *phoS* to *phoP-phoR* in the *Bacillus* genomes led us to speculate that it may be linked to PO_4^{3-} (Pi) metabolism. We presumed that *phoS* transcription might be regulated by changes in Pi levels. To test this hypothesis, we constructed a transcriptional fusion of P_{phoS}-*gfp* and integrated it into the *amyE* locus in FZB42. We recorded the fluorescence intensities (Supplementary Fig. 5a, c) and optical densities (OD_{600}) (Supplementary Fig. 5b, d) of each strain culture along growth. Since the different Pi levels strongly affected the optical density of each culture and could therefore influence the fluorescence intensity value, we calibrated the effect of Pi levels on the expression of P_{phoS}-*gfp* by comparing GFP intensity per OD of the cultures (Fig. 4a, b). We found that the fusion was expressed in a medium with 0.3 mM Pi but was not detectable if the Pi concentration was higher than 3 mM (Fig. 4a). Further studies showed that *phoS* was expressed in a dose-dependent but negatively correlated fashion in response to Pi concentrations ranging from 0.3 mM to 1.8 mM (Fig. 4b) (Supplementary Fig. 5c, d). The results of Northern blot assays further confirmed that PhoS was expressed in the presence of 0.3 mM Pi but was not detectable with 1.8 mM Pi (Fig. 4c). Therefore, we conclude that the expression of PhoS is induced by phosphate limitation.

Pi assimilation in *Bacillus* is controlled by the PhoR-PhoP two-component system. While PhoR is a sensory histidine kinase, PhoP is a cytoplasmic transcriptional regulator that is phosphorylated by PhoR upon Pi scarcity. Phosphorylated PhoP (PhoP~P) is able to bind to specific sequences of its target genes, activating or repressing their transcription[26]. In a previous work focused on a genome-wide analysis of PhoP~P binding to chromosomal DNA of *B. subtilis*[27], the authors identified four motifs (Pho box) for putative binding sites of PhoP~P at the 3' end of the *phoPR* operon, which exactly corresponds to the promoter region of *phoS* (Fig. 1d). We identified the same Pho boxes in the upstream region of *phoS* in FZB42 (Supplementary Fig. 6). Thus, we inferred that PhoP can directly target the promoter region of *phoS* and activate its transcription in response to Pi scarcity. To test this inference, we deleted *phoP* and examined its effect on *phoS* expression. The results showed that *phoP* deletion reduced the fluorescence intensity of cells carrying the P_{phoS}-*gfp* fusion (Fig. 4d). Since *phoP* deletion also decreased

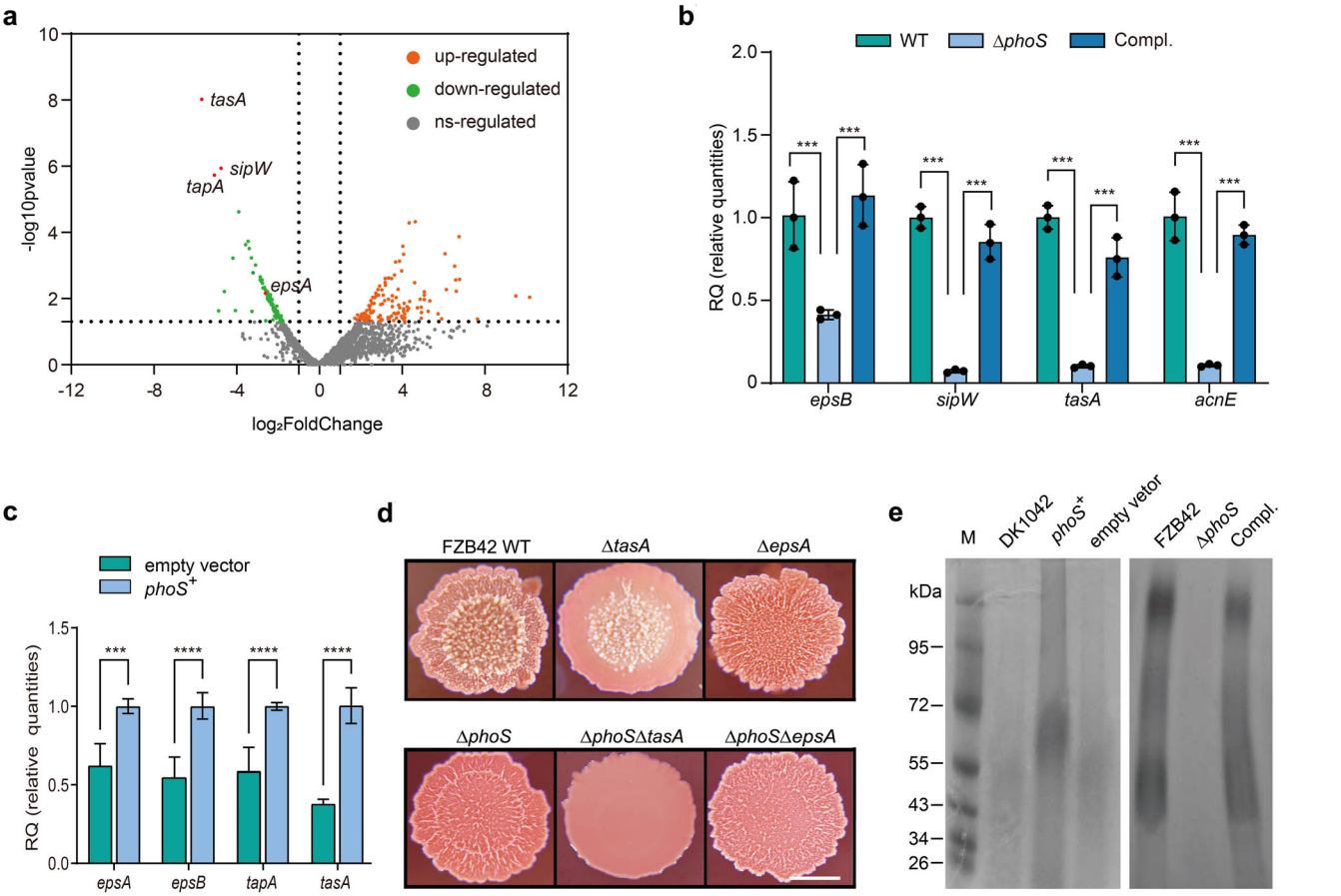

Fig. 3 | PhoS regulates genes involved in *Bacillus* biofilm formation. a DEGs between the transcriptomes of *B. velezensis* FZB42 wild type and its Δ*phoS* mutant. Total RNA was extracted 13 h after inoculation in RNB medium. Three biological replicates were used for each strain ($n = 3$) with the standard deviations indicated by the bars. **b**, **c** Verification of the transcription level of selected biofilm-related DEGs from (**a**) was verified by qPCR. **b** FBZ42 wild type, Δ*phoS* mutant and *phoS* complementation strain (Compl.) were grown in RNB medium, while (**c**) DK1042 carrying an empty vector or the overexpressed *phoS* was grown in LB. **d** Effect of *epsA*, *tasA*, and *phoS* on colony morphology of *B. velezensis* FZB42, which was grown on LB agar containing Congo red at 25 °C for 8 days before imaging. **e** Effect of *phoS* on EPS production by different strains of *B. subtilis* DK1042 and *B. velezensis* FZB42. The strains were grown in LB for 24 h before EPS extraction from the same volume of bacterial cultures and staining with Stains-all® base solution.

the OD_{600} values of the bacterial cultures (Fig. 4e), we compared the fluorescence intensity per OD of the strains (Fig. 4f), similar to what we did in Fig. 4a, b. As a set of positive controls, the expression of P_{spac}-*gfp* in the Δ*phoP* mutant was much higher than that in the *phoP*-positive strain (Fig. 4f). In contrast, the expression of P_{phoS}-*gfp* in the Δ*phoP* mutant was significantly lower than that in the *phoP* intact strain (Fig. 4f), indicating that the expression of *PhoS* indeed requires PhoP.

PhoS promotes expression of PhoP by targeting 5'UTR of *phoP* mRNA

Salzberg et al. reported that the 3' UTR of *phoR* of *B. subtilis* is required for the positive autoregulation of *phoPR* expression[27], although the underlying mechanism remains unknown. Building on our discovery of *phoS* in the 3'UTR of *phoR*, we hypothesized that PhoS may mediate the positive autoregulation of *phoPR*. To test this hypothesis, we also employed the *B. subtilis* DK1042 strain taking advantage of its amenability for plasmid transformation[23]. Our results showed that overexpression of *phoS* in DK1042 led to a more than threefold increase in *phoP* mRNA level (Fig. 5a), suggesting that PhoS can promote *phoP* expression. Meanwhile, we generated a *phoP*::*gfp* translational fusion by fusing the promoter and the coding sequence for the first 15 amino acids of PhoP to the *gfp* gene, and then introduced this construct into DK1042 carrying the plasmid for *phoS* overexpression. We conducted the assay and observed that PhoS overexpression promoted GFP expression (Fig. 5b), suggesting that PhoS can indeed increase *phoP* expression, most likely by interacting with the region we fused to *gfp*.

To validate this interaction, we determined the transcription start site (TSS) of *phoP* of FZB42 using the dRNA-seq result (Supplementary Fig. 7). With this information, we predicted[28] that the seed region of PhoS could base pairs with the +21 to +47 region in the 5′UTR of *phoP* (Fig. 5c, d). The predicted hybridization energy between the two transcripts was −20.1 kcal/mol, indicating a high degree of confidence. To evaluate this prediction, we assayed the effects of nucleotide mutations of *phoS* on *phoP* expression in DK1042. Our results revealed that changing the guanine at either the +5 or +7 position in the seed region to cytosine (C5G or C7G) did not affect the transcription of the *phoP*::*gfp* (Supplementary Fig. 8a) but abolished the promoting effect of PhoS on *phoP*::*gfp* expression, both in liquid LB (Fig. 5e) and on LB agar plates (Supplementary Fig. 8b). These effects were not due to differences in growth, since site-directed mutations in *phoS* did not affect the growth of the mutants (Supplementary Fig. 8c). We also validated this effect via Western blotting, which showed that GFP expression was barely detectable in the cells bearing the mutated *phoS* (Fig. 5f). These results further bolstered our deduction that PhoS promotes *phoP* expression by targeting the 5'UTR of *phoP* mRNA.

Additionally, we examined the transcriptome data showing the effect of PhoS on FZB42 gene expression (Supplementary Table 1). As a transcriptional regulator, PhoP orchestrates, dominantly activates, the expression of no less than 25 operons. Among the 135 down-regulated genes in the

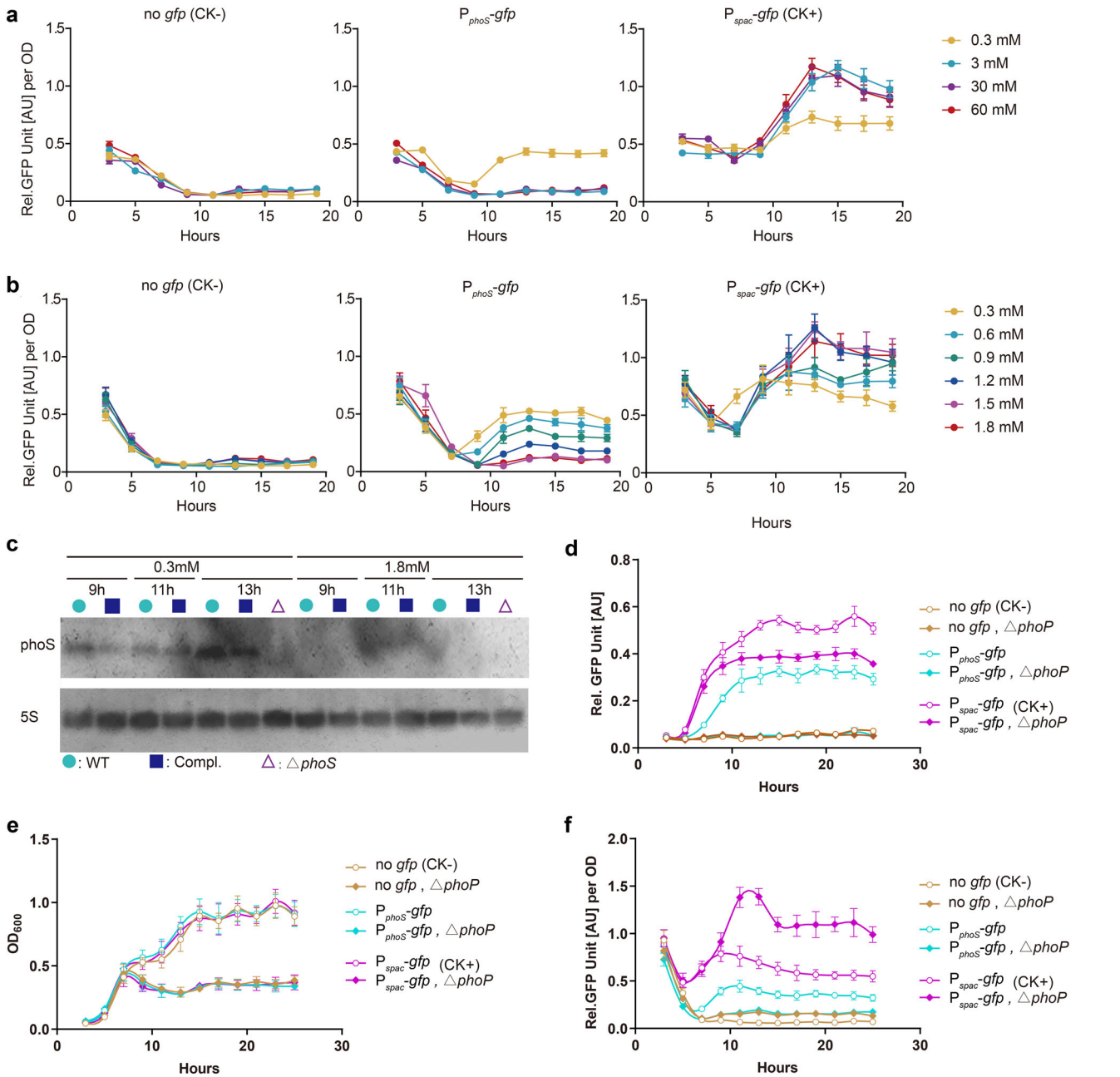

Fig. 4 | Regulation of *phoS* expression in *B. velezensis* FZB42 by phosphate and the transcriptional regulator PhoP. a, **b** Effect of phosphate concentration on the GFP fluorescence intensity per OD of FZB42 cells carrying the P_{phoS}-*gfp* fusion. The *gfp* reporter strain carrying the transcriptional fusion of P_{phoS}-*gfp* was grown under four different Pi concentrations (0.3, 3, 30, and 60 mM) in GP medium (**a**). The optical density at 600 nm (OD_{600}) of the cultures and their GFP fluorescence intensity (relative fluorescence unit, RFU) were recorded over time (Supplementary Fig. 7). The ratio of RFU to OD_{600} was calculated and plotted. The wild-type FZB42 carrying no *gfp* was used as the negative control (CK−), while a constitutively expressed P_{spac}-*gfp* fusion in the absence of *lacI* was used as the positive control (CK +) to evaluate the effect of Pi concentration on GFP protein. **b** A similar assay was performed under six different Pi concentrations (0.3, 0.6, 0.9, 1.2, 1.5, and 1.8 mM). The OD_{600} values of the cultures and their RFU values were shown over time also in Supplementary Fig. 7. **c** Northern blot showing *phoS* expression in FZB42 grown in GP medium with two different phosphate concentrations (0.3 and 1.8 mM). The PhoS transcript was detected using digoxigenin-labeled probes, and 5S rRNA was used as a loading control. Cultures were sampled at 9, 11, and 13 h after inoculation when PhoS accumulated abundantly. WT: FZB42 wild type; Compl.: the complementation strain of *phoS*. **d**–**f** Effects of *phoP* on the expression of *phoS* in FZB42. The GFP activity of P_{phoS}-*gfp* in the FZB42 wild type and the *phoP* mutant was compared by growing them in LB. The fluorescence intensity (**d**) and optical density (**e**) of the cultures were measured every 2 h for a period of 24 h, and the ratios of fluorescence RFU per OD of each strain were calculated and are shown in (**f**).

Δ*phoS* strain (Supplementary Table 1), we identified 12 genes (*pstS, pstC, pstA, pstBA; tuaA, tuaB, tuaD, tuaE, tuaF, tuaG; glpQ; dacA*), comprising four operons, whose transcription is known to be positively regulated by PhoP[27,29]. The expression of the *pst* operon and the *tua* operon decreased significantly, by approximately 4-fold and 20-fold, respectively. These results are consistent with the promoting effect of PhoS on *phoP* expression.

PhoS releases the sequestered RBS of *phoP* mRNA

To better understand how the interaction between PhoS and the *phoP* 5'UTR occurs, we predicted their interactions[30] and conducted in silico analyses and further experiments. The structural prediction for the 5'UTR of *phoP* mRNA revealed two hairpin structures (structure I and II), with one of them (structure II) sequestering the predicted RBS (Fig. 5c). Considering the

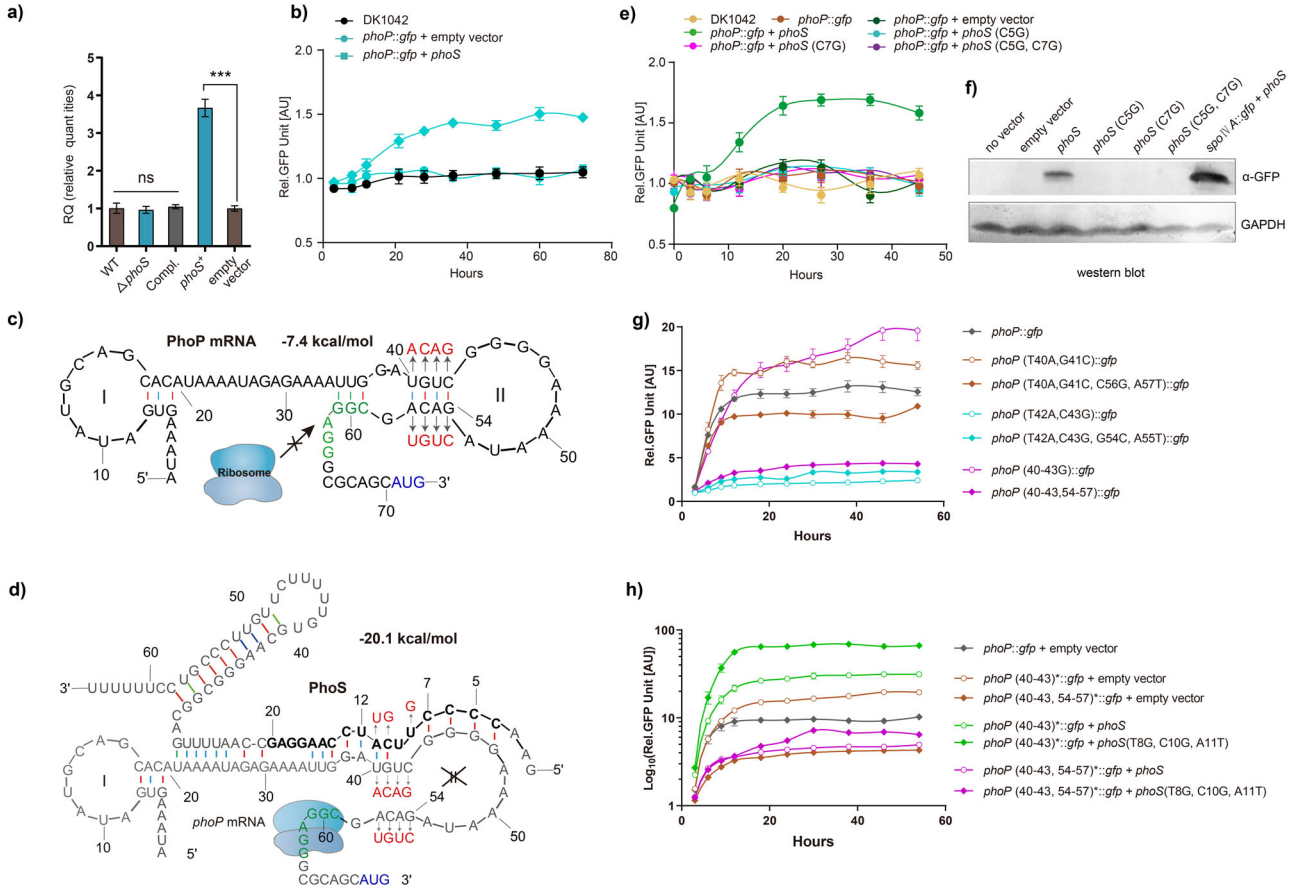

Fig. 5 | PhoS enhances *phoP* expression by releasing the sequestered RBS at the 5'UTR of *phoP* mRNA. a Effect of *phoS* overexpression on the transcription of *phoP* revealed by qPCR. *B. velezensis* FZB42 wild type, its Δ*phoS* mutant, *B. subtilis* DK1042 containing an empty vector (pDG148-stu) or the vector carrying *phoS* (pDG148-stu/*phoS*) for *phoS* overexpression were grown in LB at 37 °C for 13 h before cells were collected for RNA preparation and then qPCR. **b** Effect of *phoS* overexpression on *phoP* expression in *B. subtilis* DK1042 carrying a translational fusion *phoP::gfp*. The *phoS* gene of FZB42 was inserted in the pDG148-stu plasmid and introduced into DK1042 for constitutive expression, while the DK1042 strain carrying an empty pDG148 plasmid or no plasmid was used as a control. GFP fluorescence from the cultures of each strain was measured over time. **c** Predicted secondary structure of the 5′UTR of *phoP* mRNA with stem-loop structure II sequestering the RBS and (**d**) binding of PhoS to the 5′UTR opens up structure II and makes the RBS accessible for translation. The RBS is indicated in green, and the start codon is indicated in red. The seed region of PhoS is shaded in gray. The asterisks indicate the nucleotides that were mutated for assays in (**g**, **h**). **e**, **f** Effect of nucleotide mutations of *phoS* on *phoP* expression reported by (**e**) GFP fluorescence and by (**f**) α-GFP antibody. Glyceraldehyde-3-phosphate dehydrogenase (GAPDH) was used as the loading control. The translational fusion *spoIVA::gfp* was used as the positive control. **g**, **h** Effect of nucleotide substitutions at the stem region of structure II of the *phoP* mRNA on the activities of the *phoP::gfp* translation fusion in the absence (**g**) and presence (**h**) of *phoS* with/without compensatory nucleotide substitutions. The point substitutions are indicated in brackets; the successive substitutions in a region are indicated by an asterisk along with the brackets. The substitutions follow the principle A→T, T→A, G→C, and C→G. For (**a**, **b**, **e**, **g**, **h**), three biological replicates were measured ($n = 3$) with standard deviations indicated by the bars.

advantage that *E. coli* cells can easily maintain two compatible plasmids and high fluorescence brightness, we carried out the interaction investigation in *E. coli* (Supplementary Fig. 9). The reliability of the interaction system was determined before application (Supplementary Fig. 10). We performed nucleotide substitutions in the stem of structure II, specifically in the region from +40 to +43 (T40A, G41C, T42A, C43G), and examined their impact on *phoP* expression. We predicted that the nucleotide substitutions would weaken the stem structure, release the RBS from sequestration, and enhance *phoP* expression (Supplementary Fig. 11a, b). Indeed, the results showed that nucleotide mutations at the +40 and +41 positions (T40A/G41C) increased *phoP* expression (T40A/G41C, Fig. 5g), while compensatory changes at the +57 and +56 positions, designed to restore base pairings with the mutated +40 and +41 positions on the stem, led to lower *phoP* expression (T40A/G41C/C56G/A57T, Fig. 5g) than that of native *phoP*. None of the above nucleotide substitutions affected the growth rate of the cells Supplementary Fig. 12a). These results suggest that the native base pairing between the +40/+41 and +56/+57 nucleotides has a moderate inhibitory effect on *phoP* expression. In contrast, mutations at the +42 and +43 positions (T42A, C43G) strongly reduced *phoP* expression by approximately 5-fold (T42A/C43G, Fig. 5g). Moreover, their compensatory nucleotide substitutions at the +55 and +54 positions, which were designed to restore the base pairings on the stem, could not restore *phoP* expression at all (Fig. 5g). This result is probably because the RBS is sequestered by a newly formed stem-loop structure after the mutations at the +42 and +43 positions (Supplementary Fig. 11c). Similar to the mutations at the +40 and +41 positions, mutations in the entire region from +40 to +43 nucleotides also led to a clear promotion of *phoP* expression, while the compensatory nucleotide changes at the region from +57 to +54 again strongly reduced *phoP* expression (Fig. 5g). As a set of controls, we also made mutations at some relative trivial positions shown in the structure prediction and examined their effect. For example, nucleotide changes were created at the +66 and +68 positions (C66G/C68G). We found that these mutations did not significantly alter the expression of *phoP* (Supplementary Fig. 12b, c), which countered the importance of +40 to +43 and +54 to +57. Finally, we measured GFP fluorescence intensity from bacterial colonies on agar plates and obtained similar results (Supplementary Fig. 12c) to those obtained in the liquid media above. Collectively, our results suggest that structure II indeed exert an inhibitory effect on *phoP* expression.

We also predicted the interaction between PhoS and the 5'UTR of *phoP* and proposed that binding of PhoS (through the seed region) to the +21 to +47 region of the 5'UTR of *phoP* mRNA could open up the inhibitory structure II, which sequesters the RBS and thus allows translation of *phoP* (Fig. 5d). To validate this hypothesis, we generated nucleotide mutations in *phoS* and tested the impact of these mutations on *phoP* expression (Fig. 5h). In the presence of an empty vector containing no *phoS*, nucleotide mutations at the +40 to +43 region significantly increased *phoP*::*gfp* expression compared to *phoP*::*gfp* without mutations [for simplicity, the expression ($_{phoP\ (40\text{-}43)^*::gfp\ with\ empty\ vector}$) was higher than the expression ($_{phoP::gfp\ with\ empty\ vector}$), where * indicates nucleotide substitution. We use this indication hereafter for convenience]. In contrast, the compensatory changes at the +57 to +54 positions designed to restore base pairings with the mutated nucleotides at the +40 to +43 positions substantially decreased *phoP* expression [the expression ($_{phoP\ (40\text{–}43,\ 54\text{–}57)^*::gfp\ with\ empty\ vector}$)] (Fig. 5h). This finding is consistent with the result above in the absence of the empty vector, suggesting that the inhibition of structure II persisted well in the presence of the empty vector. When PhoS was present, the expression of *phoP* with mutations in the +40 to +43 region was higher than that with only the empty vector [the expression ($_{phoP\ (40\text{-}43)^*::gfp\ with\ phoS}$) was higher than the expression ($_{phoP\ (40\text{-}43)^*::gfp\ with\ empty\ vector}$)] (Fig. 5h), indicating that PhoS still to some extent functioned because its other nucleotides binding to *phoP* mRNA remained. Notably, while the mutations at the +40 to +43 region disable the base pairings at the +40 and +41 positions, they lead to two new base pairings at the +42 and +43 positions. Since the nucleotide mutations at the +40 to +43 region should completely disrupt structure II, a possible explain for the promotion effect of *phoS* in this situation is that PhoS can increase the stability of *phoP* mRNA. When the compensatory changes at +57 to +54 were introduced, the presence of PhoS could no longer improve *phoP* expression, resulting in a GFP level similar to the effect of the empty vector [the expression ($_{phoP\ (40\text{–}43,\ 54\text{–}57)^*::gfp\ with\ phoS}$) was equal to the expression ($_{phoP\ (40\text{–}43,\ 54\text{–}57)^*::gfp\ with\ empty\ vector}$)] (Fig. 5h). This should be because structure II swapped two parts of its stem sequences such that the native PhoS could no longer bind to it tightly enough to open the stem. However, when we mutated the nucleotides at the 8th, 10th, and 11th positions of PhoS to establish consecutive base pairings with the altered nucleotides at the +40 to +43 positions, *phoP*::*gfp* expression increased by ~1.8-fold compared with that when PhoS was not mutated [the expression ($_{phoP\ (40\text{-}43,\ 54\text{-}57)^*::gfp\ with\ phoS\ (T8G,\ C10G,\ A11T)}$) was higher than the expression ($_{phoP\ (40\text{-}43,\ 54\text{-}57)^*::gfp\ with\ phoS}$)] (Fig. 5h), suggesting that the mutated PhoS had a recovered, actually stronger, promoting effect on the expression of the mutated *phoP* (Fig. 5h). The highest level of *phoP* expression was observed when both the nucleotides at the 8th, 10th, and 11th position of PhoS and the nucleotides at the +40 to +43 region of *phoP* were mutated but without compensatory mutations at the +57 to +54 region, that is, the GFP expression ($_{phoP\ (40\text{-}43)^*::gfp\ with\ phoS\ (T8G,\ C10G,\ A11T)}$) was the highest (Fig. 5h). This result further support for our presumptions proposed above: specifically, the mutations on the stem of inhibitory structure II disrupted its function, while the mutated PhoS stabilized the mutated *phoP* mRNA through restored base paring.

We also investigated the interaction between PhoS and *phoP* carrying mutations at the +40 and +41 positions. We found that the expression of *phoP* carrying these mutations, with or without PhoS, fell within a narrow range. Although slightly higher than the native *phoP*, they were barely significantly differed among them (suppl. info. Supplementary Fig. 12d). This result suggests that only two mutations in the stem region could not effectively reflect the mechanism underpinning the PhoS- *phoP* mRNA interaction.

Discussion

In this study, we identified PhoS, a 3'UTR-derived sRNA that is induced in expression by environmental phosphate deprivation while regulating biofilm formation in *Bacillus*. PhoS is highly conserved in the species complex of *Bacillus*, a group of species including many agriculturally and industrially important strains as well as the model microorganism *B. subtilis* 168. Based on our results, we propose a model for the regulation of *Bacillus* phosphorus homeostasis and biofilm formation by PhoS (Fig. 6): Under Pi-limiting conditions, the transcriptional regulator PhoP enhances the expression of PhoS, which in turn promotes the translation of *phoP* mRNA by preventing the inhibitory structure at its 5'UTR that sequesters the RBS. These two regulations constitute an autoregulatory loop that is self-reinforcing. The loop could lead to a sensitive response to Pi scarcity, allowing *Bacillus* to dynamically adapt to Pi levels in the environment. Meanwhile, PhoS can affect biofilm development via the PhoP regulon: PhoP regulates the expression of over twenty operons, several of which have been shown to be required for *Bacillus* biofilm formation[31,32]. These operons include the genes involved in cell wall metabolism in adaption to phosphate limitation, such as those for biosynthesis of teichoic acids and teichuronic acids. Teichoic acids are essential polymers embedded in peptidoglycans of cell walls of gram-positive bacteria. Under phosphate limitation, PhoP~P leads to repression of the *tagAB* operon, which is responsible for biosynthesis of teichoic acids, and activation of the *tuaA-H* operon, which produces higher levels of teichuronic acids that take over the function of teichoic acids. *Bucher* et al. showed that the deletion of *tuaH* results in a clear defect in biofilm formation of *B. subtilis*[31]. In this study, we found that the expression of the *tuaA-H* operon was strongly decreased by *phoS* deletion (Supplementary Table 1, Supplementary Fig. 13a). Therefore, we conclude that PhoS can promote biofilm formation through the regulation of the *tuaA-H* operon by PhoP (Fig. 6).

However, while it is straightforward to understand the regulation of biofilm formation by PhoS through teichuronic acid biosynthesis, we do not exclude the possibility that other targets of PhoS or other regulatory circuits are also involved. For example, in the PhoP regulon there are more genes which can influence biofilm formation. One is the gene *comQ*, which encodes encoding isoprenyl transferase, a prenylation enzyme for quorum sensing. The binding of PhoP has been identified in the promoter region of *comQ*, whose expression was induced 150- to 250-fold in a PhoPR-dependent manner upon phosphate limitation[27]. Since *comQ* is the first gene of the *comQ-X-P-A* operon, we infer that PhoP may also positively regulate the expression of *comA*. Phosphorylated ComA (ComA~P) binds to the promoters of its target genes[33], such as *degQ* and the *srf* operon (*srfAA-srfAB-comS-srfAC-srfAD*). Both *degQ* and the surfactin-producing *srf* operon are involved in biofilm development. For *degQ*, its product DegQ increases the phosphorylation rate of the global transcriptional regulator, DegU[34], which regulates both biofilm formation and spore development[35–37]; while surfactin is an inducer of *Bacillus* biofilm, triggering biofilm matrix production by indirectly activating the sensor kinase KinC and then the master regulator Spo0A[38,39]. Hence, the regulation of *comQ-X-P-A* by PhoP may allow PhoS to positively regulate biofilm development either through DegU~P activity, the surfactin signaling pathway, or both pathways simultaneously (Fig. 6). Additionally, the expression of the *srf* operon is also directly, but slightly, activated by PhoP[27,40]. This means that PhoS can also indirectly promote biofilm formation through PhoP and then surfactin production (Fig. 6).

Currently, we do not know to what extent each of these pathways contributes to the regulation of biofilm by PhoS. We speculate that the signaling pathway mediated by surfactin, Spo0A~P and SinI may be important because it can directly stimulate the expression of the *eps* operon and the *tapA-sipW-tasA* operon, which can easily explain our finding that PhoS enhances their expression (Fig. 3). While we did observe decreased expression of *comQ* and *comA* in the Δ*phoS* mutant (Supplementary Fig. 13b, c), we did not find a significant difference between the transcription of the *srf* operons in the FZB42 wild type and that in the Δ*phoS* mutant (Supplementary Fig. 13d). We neither detected a significant difference in surfactin production between the FZB42 wild-type and the Δ*phoS* mutant (Supplementary Fig. 14). The reason for the inconsistence remains unknown. This is probably because surfactin producers account for only ~3% of the cell population[41]; thus, the impact of ComA was diluted to an extent that cannot be detected. However, while the pathway from ComA to Spo0A~P may function in FZB42 and DK1042, there must be an additional

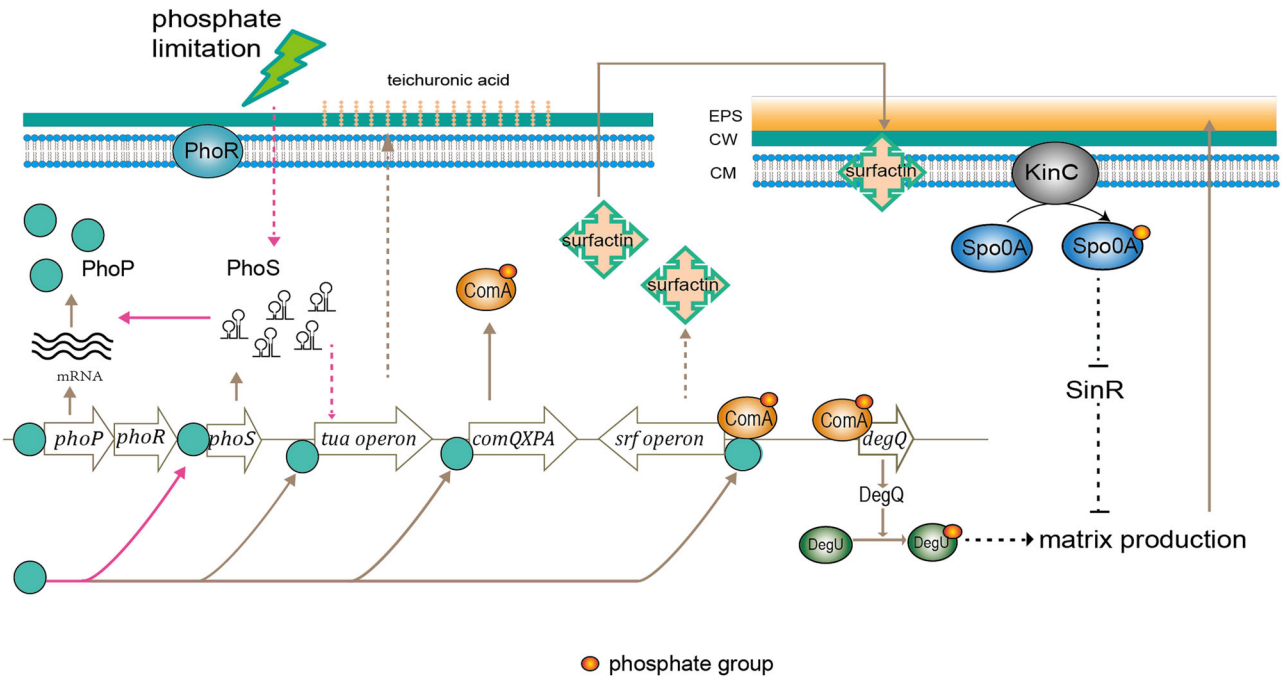

Fig. 6 | Schematic of the regulation of *Bacillus* biofilm formation by the sRNA PhoS and its transcription upon phosphate limitation. The expression of PhoS requires the transcriptional regulator PhoP, whose translation is promoted by PhoS, which forms an autoregulation loop. PhoP binds to the promoter regions the *srf* operon and the *comQXPA* operon, activating their transcription. ComA stimulates surfactin production and the expression of *degQ*. Surfactin-producing cells themselves do not produce extracellular matrix, but rather another subpopulation responds to surfactin and produces extracellular matrix[38]. ComA positively regulates biofilm formation via Spo0A. The pink lines indicate the regulations which were experimentally demonstrated in this study, while the lines in other color show the regulations which are from literatures and speculatively function in the regulation of biofilm formation by PhoS. The dashed lines indicate indirect regulation. The length of the genes or operons illustrated here is not proportional to their actual size, nor are their positions exactly consistent with their relative locations in the FZB42 genome. EPS: extracellular polymeric substances (matrix); CW: cell wall; CM: cell membrane.

mechanism to explain the regulation by PhoS in the *B. subtilis* 168 strain. Like many other 168 strains used different labs[42], our 168 strain is unable to form robust biofilm because of mutations in four genes: *epsC*, *sfp*, *degQ*, and *swrA*[6]. The mutations in the first three genes lead to inability to produce EPS, surfactin, and lowered activity of DegU~P, respectively, all of which are associated with biofilm formation. Therefore, the promoting effect of PhoS on biofilm formation in 168 should be attributed to alternative factors. The influence of PhoS on cell wall component teichuronic acids, operating through an independent pathway, offers a plausible rationale.

Within the PhoP regulon, PhoP represses three genes (*tagD, tagE, ggaA*) involved in teichoic acid synthesis, which have also reported to impact biofilm formation[31,32]. However, we did not detect a significant difference in their expression between the FZB42 wild type and the Δ*phoS* mutant. This is probably because they are repressed, rather than stimulated, by PhoP or their fold change is much lower than that of the *tua* operon[43], which thus falls below the threshold that required for robust detection by transcriptomic analysis.

Notably, the impact of *phoS* deletion on both biofilm formation (Fig. 2b–d) was relatively weak, whereas the effect of *phoS* overexpression on biofilm formation (Fig. 2a) was strong. This discrepancy may have at least one reason: the regulatory relay "PhoS, *phoP* mRNA, PhoP, *phoS*, PhoS" forms a self-reinforcing autoregulatory loop. When *phoS* is overexpressed, the loop could lead to a rapid accumulation of PhoP and thus promote biofilm development. For this reason, the effect of *phoS* overexpression on biofilm formation would be much more noticeable than that of *phoS* deletion.

The transcriptome analysis also revealed significant changes in the *eps* and *tapA-sipW-tasA* operons upon deletion of *phoS* (Fig. 3a). Given their well-known roles in biofilm formation, we investigated the potential of PhoS to directly target them using the methods and system developed above. Although the IntaRNA algorithm[44] predicted strong binding sites for PhoS within their 5'UTRs, our results demonstrated that neither of these two operons are direct targets of PhoS (Supplementary Fig. 15).

It should be noted that we used *E. coli* to validate the interaction between PhoS and *phoP* mRNA. While this heterologous system offers many advantages such as brighter fluorescence, easier genetic manipulation, and higher adaptability to other target detection, it may also lead to unexpected artifacts. For instance, unlike the situation in *Bacillus*[45], the RNA chaperone Hfq in *E. coli* has a strong interaction with sRNAs. Therefore, appropriate control sets are crucial to the investigations utilizing the heterologous system. Meanwhile, we evaluated the potential interaction between *E. coli* Hfq and PhoS. By using DsrA as a positive control[46], we revealed that Hfq does not bind to PhoS in *E. coli* (Supplementary Fig. 16). We speculate that PhoS may lack some specific motifs or sequences recognized by *E. coli* Hfq. The short length of PhoS may also affect its binding affinity for Hfq. To further analyze the possible difference between the *B. subtilis* and the *E. coli* systems for target validation, we conducted the similar experiment with *E. coli* as in *B. subtilis* (Fig. 5e). The result showed that the G7C single point mutation of PhoS did not affect its regulatory function on *phoP*::*gfp* expression, whereas the G5C single point mutation significantly reduced, and the double mutations (C7G and C5G) almost abolished, the regulatory function (Supplementary Fig. 17). This outcome is not identical to the regulatory effect of PhoS in *Bacillus* (Fig. 5e), where even a single point mutation completely eliminated its regulatory effect. In comparison, the GFP fluorescence is much stronger in *E, coli*, while the regulatory role of PhoS appears to be more sensitive to the mutations in *B. subtilis* for unknown reasons. Therefore, although the *E. coli* system offers advantages, results obtained from it should be interpreted with caution.

In summary, as a model organism for gram-positive bacteria, *B. subtilis* has been thoroughly examined for sRNA candidates[47–49], most of

which have unknown functions. While sRNAs are known to modulate many aspects of bacterial metabolism, their roles in *Bacillus* Pi metabolism and multicellular behavior, such as biofilm formation, have barely been investigated. In this context, PhoS represents one of the best-studied *Bacillus* sRNAs and is involved in these critical biological processes. In the future, there are still some issues that should be addressed. For example, it is necessary to explore whether additional mRNAs are targeted by PhoS and whether other *Bacillus* characteristics, such as sporulation and competence, are affected by PhoS. It would also be interesting to explore whether other environmental cues affect PhoS expression and how PhoS orchestrates the expression of a myriad of genes in a complex environment such as the rhizosphere. In particular, how PhoS integrates its functions in response to phosphate accessibility can be a crucial avenue for future research.

Methods

Bacterial strains, media and growth conditions

The bacterial strains constructed in this study are listed in Supplementary Table 2. Details on the validation of PhoS target in *E. coli* and *B. subtilis* are provided in Supplementary Fig. 9, 10.

B. subtilis and *B. velezensis* strains were grown in different media, including conventional lysogeny broth (LB), LBGM medium [LB with 1% (v/v) glycerol and 0.1 mM $MnSO_4$], LBGM-YE medium [10 g tryptone, 5 g NaCl per L, 1% (v/v) glycerol and 0.1 mM $MnSO_4$], MSgg medium[8], and RNB medium (10 g tryptone, 1 g yeast extract, 5 g NaCl per L), as well as on medium plates fortified with 1.5% (w/v) Bacto agar. GP medium was also used with different concentrations of KH_2PO_4 as indicated[29]. The four media used in the differential sequencing experiment were as follows: i) 1CM medium, ii) 1CM medium with maize root exudates (+RE), iii) 1CM medium with soil extract (+SE), and iv) 1CM medium with both maize root exudates and soil extract (+RS), as previously reported[22]. As necessary, antibiotics were added at the following concentrations: 100 μg/mL ampicillin, 100 μg/mL spectinomycin, 5 μg/mL kanamycin, and 1 μg/mL erythromycin plus 25 μg/mL lincomycin.

Oligonucleotides and plasmids

The list of DNA oligonucleotides and plasmids used in this study can be found in Supplementary Tables 3 and 4. Details on plasmid construction are provided in the Supplementary Materials and Methods section.

Construction of mutant strains

Chromosomal manipulation of *B. velezensis* FZB2 and *B. subtilis* DK1042 was performed as previously described[50]. For constructing the *phoS* deletion strain (FBS22), pFB22 was transformed into wild-type FZB42 for homologous recombination. Correct transformants were screened by corresponding antibiotic selection and verified by colony PCR and DNA sequencing.

For target verification in *Bacillus*, plasmids carrying a *target*::*gfp* translational fusion (or a mutated *target*::*gfp*) with the *amyE* flanking sequences were transformed into DK1042 for homologous recombination. Then, the plasmid pDG148-stu, harboring the *phoS* gene (or a mutated variant of *phoS*), was introduced into the recombinant strains above for GFP fluorescence quantification. For the validation of a PhoS target in *E. coli*, the plasmid (pXG-10) carrying a fusion sequence of *target*::*gfp* (or a mutated *target*::*gfp*) and the plasmid pDG148-stu carrying the *phoS* gene (or a mutated variant of *phoS*) were transformed into *E. coli* Top10. As a control, pDG148-stu carrying the terminator sequence of PhoS was employed as an "empty" vector and transformed into the *B. subtilis* DK1042 or *E. coli* Top10 strains. Other integrative plasmids, such as those for the transcriptional fusion P_{phoS}::*gfp*, were similarly transformed into the *Bacillus* strains for expression from the *amyE* locus. The host strains used, the plasmids for transformation, and the primers for colony PCR or DNA sequencing verification are listed in Supplementary Tables 2–4.

RNA isolation and Northern blotting

RNA isolation and Northern blotting were performed with digoxigenin-labeled probes as previously reported[50] or with radiolabeled probes as described in a previous report[51].

RNA sequencing

The FZB42 wild-type and FBS22 (Δ*phoS*) were grown in RNB medium for 13 h before the cells were harvested for total RNA preparation using a previously described method[50]. RNA sequencing was performed at Shanghai Personal Biotechnology Co., Ltd. (China). Three independent experiments were conducted for RNA preparation and sequencing. The RNAs prepared in the first experiment were sequenced with the sequencer Illumina NextSeq 500, while those from the second and third experiments were sequenced with the sequencer Illumina HiSeq. The transcriptome data from the three experiments were comprehensively analyzed with the DESeq2 software[52].

Quantitative PCR

Total RNA was extracted using the previously described method[50]. Purified RNA was subjected to qPCR using the TB Green® Premix Ex Taq kit (TaKaRa, Japan) and the StepOnePlus™ Real-Time PCR System (ABI, USA) following the manufacturer's instructions. Gene-specific primers were designed using the Oligo 7 software (Molecular Biology Insights, Inc. USA). The housekeeping gene *gyrA* was used as the internal standard. For each assay, three biological replicates and triple or quartic technical repeats were conducted. Sequences of all primers used are provided in Supplementary Table 4. The relative expression levels were estimated from the threshold of PCR cycle using the $2^{-\Delta\Delta Ct}$ method.

Colony biofilm and pellicle formation

Overnight bacterial cultures were diluted with their corresponding media to an OD_{600} of approximately 1.0. For colony biofilm formation, 3 μL of diluted cultures of each strain was spotted onto an agar plate. For pellicle formation, a 1% (v/v) inoculum was added to the liquid media in a 24-well plate. The plates were incubated at 20–25 °C over time (see figure legends for specific information on each experiment). Biofilm staining was performed as appropriate with the addition of 20 μg/mL Congo Red and/or 10 μg/mL Coomassie Brilliant Blue G250 to the media. Visualization was performed with the FluorChem Q imager.

EPS preparation

We followed a protocol as previously reported[53] with minor modifications for EPS preparation. Briefly, bacterial strains were grown in LB with 10 mM $MgSO_4$ and 100 μM $MnSO_4$ for 24 h before centrifugation. The resulting supernatant was collected and subsequently digested with RNase, DNase and proteinase K before being cooled on ice. The cooled supernatant was precipitated with 75% (v/v) cold ethanol and centrifuged at 14,000 rpm for 3 min to obtain the EPS pellets. The EPS was then dissolved in 1× SDS buffer. Ten microliters of the dissolved EPS were loaded onto a 12% (v/v) SDS-PAGE gel. After electrophoresis, the gel was fixed with 25% (v/v) isopropanol and 3% (w/v) acetic acid for 24 h and stained with 100 mL of Stain-all® reactive solution. The stacking gel was imaged using the FluorChem Q imager.

GFP fluorescence quantification

For each strain, three colonies were randomly selected for preculture overnight and were then adjusted to the same concentration before being inoculated (1%, v/v) into new media for incubation. For visualization and analysis of GFP fluorescence from bacterial colonies, the FluorChem Q imager was used with the excitation light set at 475 nm for excitation and emission light collection at 537/26 nm. For measurement of GFP fluorescence from liquid culture, one mL of bacterial culture was transferred to a 24-well plate, and fluorescence was quantified using a spectrophotometer (Varioskan Flash, Thermo, USA) with excitation at 480 nm and emission at 509 nm. In most cases, the GFP fluorescence intensity of different cultures

was directly plotted for comparison since their optical density values at 600 nm (OD_{600}) were similar. Under the conditions that the growth of bacteria was significantly affected by different levels of Pi in the media, GFP fluorescence intensity per OD of the cultures was compared to avoid the effect of cell density on fluorescence intensity.

Data availability

The raw data for the transcriptomes of FZB42 and FBS22 (Δ*phoS*) are available in the SRA database with the accession number SRP410781.

Received: 16 November 2023; Accepted: 13 October 2024;
Published online: 29 October 2024

References

1. Hulett, F. M. in *Bacillus subtilis and Other Gram-positive Bacteria : Biochemistry, Physiology and Molecular Biology* (eds Sonenshein, A. L., Hoch, J. A. & Losick, R.) 229–235 (American Society for Microbiology, 1993).
2. Pedreira, T., Elfmann, C. & Stülke, J. The current state of Subti Wiki, the database for the model organism Bacillus subtilis. *Nucleic Acids Res.* **50**, D875–D882 (2022).
3. Martín, J. F. Phosphate control of the biosynthesis of antibiotics and other secondary metabolites is mediated by the PhoR-PhoP system: an unfinished story. *J. Bacteriol.* **186**, 5197–5201 (2004).
4. Jia, T. et al. The phosphate-induced small RNA EsrL promotes E. coli virulence, biofilm formation, and intestinal colonization. *Sci. Signal.* **16**, eabm0488 (2023).
5. Arnaouteli, S., Bamford, N. C., Stanley-Wall, N. R. & Kovacs, A. T. Bacillus subtilis biofilm formation and social interactions. *Nat. Rev. Microbiol.* **19**, 600–614 (2021).
6. Vlamakis, H., Chai, Y., Beauregard, P., Losick, R. & Kolter, R. Sticking together: building a biofilm the Bacillus subtilis way. *Nat. Rev. Microbiol.* **11**, 157–168 (2013).
7. Böhning, J. et al. Donor-strand exchange drives assembly of the TasA scaffold in Bacillus subtilis biofilms. *Nat. Commun.* **13**, 7082 (2022).
8. Branda, S. S., Gonzalez-Pastor, J. E., Ben-Yehuda, S., Losick, R. & Kolter, R. Fruiting body formation by *Bacillus subtilis*. *Proc. Natl Acad. Sci. USA* **98**, 11621–11626 (2001).
9. Kearns, D. B., Chu, F., Branda, S. S., Kolter, R. & Losick, R. A master regulator for biofilm formation by *Bacillus subtilis*. *Mol. Microbiol.* **55**, 739–749 (2005).
10. Romero, D., Aguilar, C., Losick, R. & Kolter, R. Amyloid fibers provide structural integrity to Bacillus subtilis biofilms. *Proc. Natl Acad. Sci. USA* **107**, 2230–2234 (2010).
11. Jackson, D. W. et al. Biofilm formation and dispersal under the influence of the global regulator CsrA of Escherichia coli. *J. Bacteriol.* **184**, 290–301 (2002).
12. Lapouge, K., Schubert, M., Allain, F. H. & Haas, D. Gac/Rsm signal transduction pathway of gamma-proteobacteria: from RNA recognition to regulation of social behaviour. *Mol. Microbiol.* **67**, 241–253 (2008).
13. Mika, F. et al. Targeting of csgD by the small regulatory RNA RprA links stationary phase, biofilm formation and cell envelope stress in Escherichia coli. *Mol. Microbiol.* **84**, 51–65 (2012).
14. Monteiro, C. et al. Hfq and Hfq-dependent small RNAs are major contributors to multicellular development in Salmonella enterica serovar Typhimurium. *RNA Biol.* **9**, 489–502 (2012).
15. Thomason, M. K., Fontaine, F., De Lay, N. & Storz, G. A small RNA that regulates motility and biofilm formation in response to changes in nutrient availability in Escherichia coli. *Mol. Microbiol.* **84**, 17–35 (2012).
16. Papenfort, K., Förstner, K. U., Cong, J. P., Sharma, C. M. & Bassler, B. L. Differential RNA-seq of Vibrio cholerae identifies the VqmR small RNA as a regulator of biofilm formation. *Proc. Natl Acad. Sci. USA* **112**, E766–E775 (2015).
17. Bak, G. et al. Identification of novel sRNAs involved in biofilm formation, motility, and fimbriae formation in Escherichia coli. *Sci. Rep.* **5**, 15287 (2015).
18. Raad, N., Tandon, D., Hapfelmeier, S. & Polacek, N. The stationary phase-specific sRNA FimR2 is a multifunctional regulator of bacterial motility, biofilm formation and virulence. *Nucleic Acids Res.* **50**, 11858–11875 (2022).
19. Bronesky, D. et al. A multifaceted small RNA modulates gene expression upon glucose limitation in Staphylococcus aureus. *EMBO J.* **38**, e99363 (2019).
20. Schoenfelder, S. M. K. et al. The small non-coding RNA RsaE influences extracellular matrix composition in Staphylococcus epidermidis biofilm communities. *PLoS Pathog.* **15**, e1007618 (2019).
21. Fan, B., Blom, J., Klenk, H. P. & Borriss, R. Bacillus amyloliquefaciens, Bacillus velezensis, and Bacillus siamensis Form an "Operational Group B. amyloliquefaciens" within the B. subtilis Species Complex. *Front. Microbiol.* **8**, 22 (2017).
22. Fan, B. et al. dRNA-Seq reveals genomewide TSSs and noncoding RNAs of plant beneficial Rhizobacterium Bacillus amyloliquefaciens FZB42. *PLoS One* **10**, e0142002 (2015).
23. Konkol, M. A., Blair, K. M. & Kearns, D. B. Plasmid-encoded comi inhibits competence in the ancestral 3610 strain of Bacillus subtilis. *J. Bacteriol.* **195**, 4085–4093 (2013).
24. Joseph, P., Fantino, J. R., Herbaud, M. L. & Denizot, F. Rapid orientated cloning in a shuttle vector allowing modulated gene expression in Bacillus subtilis. *FEMS Microbiol. Lett.* **205**, 91–97 (2001).
25. Arnaouteli, S., MacPhee, C. E. & Stanley-Wall, N. R. Just in case it rains: building a hydrophobic biofilm the Bacillus subtilis way. *Curr. Opin. Microbiol.* **34**, 7–12 (2016).
26. Pragai, Z. et al. Transcriptional regulation of the phoPR operon in Bacillus subtilis. *J. Bacteriol.* **186**, 1182–1190 (2004).
27. Salzberg, L. I. et al. Genome-wide analysis of phosphorylated PhoP binding to chromosomal DNA reveals several novel features of the PhoPR-mediated phosphate limitation response in Bacillus subtilis. *J. Bacteriol.* **197**, 1492–1506 (2015).
28. Busch, A., Richter, A. S. & Backofen, R. IntaRNA: efficient prediction of bacterial sRNA targets incorporating target site accessibility and seed regions. *Bioinformatics* **24**, 2849–2856 (2008).
29. Antelmann, H., Scharf, C. & Hecker, M. Phosphate starvation-inducible proteins of Bacillus subtilis: proteomics and transcriptional analysis. *J. Bacteriol.* **182**, 4478–4490 (2000).
30. Zuker, M. Mfold web server for nucleic acid folding and hybridization prediction. *Nucleic acids Res.* **31**, 3406–3415 (2003).
31. Bucher, T., Oppenheimer-Shaanan, Y., Savidor, A., Bloom-Ackermann, Z. & Kolodkin-Gal, I. Disturbance of the bacterial cell wall specifically interferes with biofilm formation. *Environ. Microbiol. Rep.* **7**, 990–1004 (2015).
32. Xu, Z. et al. Bacillus velezensis wall Teichoic acids are required for biofilm formation and root colonization. *Appl. Environ. Microbiol.* **85**, e02116–18 (2019).
33. Core, L. & Perego, M. TPR-mediated interaction of RapC with ComA inhibits response regulator-DNA binding for competence development in Bacillus subtilis. *Mol. Microbiol.* **49**, 1509–1522 (2003).
34. Msadek, T., Kunst, F., Klier, A. & Rapoport, G. DegS-DegU and ComP-ComA modulator-effector pairs control expression of the Bacillus subtilis pleiotropic regulatory gene degQ. *J. Bacteriol.* **173**, 2366–2377 (1991).
35. Kobayashi, K. Gradual activation of the response regulator DegU controls serial expression of genes for flagellum formation and biofilm formation in Bacillus subtilis. *Mol. Microbiol.* **66**, 395–409 (2007).

36. Marlow, V. L. et al. Phosphorylated DegU manipulates cell fate differentiation in the Bacillus subtilis biofilm. *J. Bacteriol.* **196**, 16–27 (2014).
37. Verhamme, D. T., Murray, E. J. & Stanley-Wall, N. R. DegU and Spo0A jointly control transcription of two loci required for complex colony development by Bacillus subtilis. *J. Bacteriol.* **191**, 100–108 (2009).
38. Lopez, D., Vlamakis, H., Losick, R. & Kolter, R. Paracrine signaling in a bacterium. *Genes Dev.* **23**, 1631–1638 (2009).
39. Lopez, D., Fischbach, M. A., Chu, F., Losick, R. & Kolter, R. Structurally diverse natural products that cause potassium leakage trigger multicellularity in Bacillus subtilis. *Proc. Natl Acad. Sci. USA* **106**, 280–285 (2009).
40. Allenby, N. E. et al. Genome-wide transcriptional analysis of the phosphate starvation stimulon of Bacillus subtilis. *J. Bacteriol.* **187**, 8063–8080 (2005).
41. Schoenborn, A. A. et al. Defining the expression, production, and signaling roles of specialized metabolites during Bacillus subtilis differentiation. *J. Bacteriol.* **203**, e0033721 (2021).
42. Gallegos-Monterrosa, R., Mhatre, E. & Kovács, Á. T. Specific Bacillus subtilis 168 variants form biofilms on nutrient-rich medium. *Microbiology (Reading)* **162**, 1922–1932 (2016).
43. Botella, E. et al. Cell envelope gene expression in phosphate-limited Bacillus subtilis cells. *Microbiology* **157**, 2470–2484 (2011).
44. Mann, M., Wright, P. R. & Backofen, R. IntaRNA 2.0: enhanced and customizable prediction of RNA-RNA interactions. *Nucleic Acids Res.* **45**, W435–W439 (2017).
45. Rochat, T. et al. Tracking the elusive function of Bacillus subtilis Hfq. *PLoS ONE* **10**, e0124977 (2015).
46. Sledjeski, D. D., Whitman, C. & Zhang, A. Hfq is necessary for regulation by the untranslated RNA DsrA. *J. Bacteriol.* **183**, 1997–2005 (2001).
47. Irnov, I., Sharma, C. M., Vogel, J. & Winkler, W. C. Identification of regulatory RNAs in Bacillus subtilis. *Nucleic Acids Res.* **38**, 6637–6651 (2010).
48. Nicolas, P. et al. Condition-dependent transcriptome reveals high-level regulatory architecture in Bacillus subtilis. *Science* **335**, 1103–1106 (2012).
49. Mars, R. A. et al. Small regulatory RNA-induced growth rate heterogeneity of Bacillus subtilis. *PLoS Genet.* **11**, e1005046 (2015).
50. Fan, B. et al. New SigD-regulated genes identified in the rhizobacterium Bacillus amyloliquefaciens FZB42. *Biol. Open* **5**, 1776–1783 (2016).
51. Chao, Y., Papenfort, K., Reinhardt, R., Sharma, C. M. & Vogel, J. An atlas of Hfq-bound transcripts reveals 3' UTRs as a genomic reservoir of regulatory small RNAs. *EMBO J.* **31**, 4005–4019 (2012).
52. Anders, S. & Huber, W. Differential expression analysis for sequence count data. *Genome Biol.* **11**, R106 (2010).
53. Guttenplan, S. B., Blair, K. M. & Kearns, D. B. The EpsE flagellar clutch is bifunctional and synergizes with EPS biosynthesis to promote Bacillus subtilis biofilm formation. *PLoS Genet.* **6**, e1001243 (2010).
54. Markham, N. R. & Zuker, M. UNAFold: software for nucleic acid folding and hybridization. *Methods Mol. Biol.* **453**, 3–31 (2008).

Acknowledgements

The authors thank Prof. Daniel B. Kearns for generously providing *B. subtilis* DK1042 and Dr. Daniel Lopez for providing the *B. subtilis* mutants. We are also grateful to Dr. Yanjie Chao and Prof. Jörg Vogel for their critical suggestions and help in the RNA work. This study is funded by the National Key R&D Program of China (2023YFD1401304, 2021YFD1400300) and the National Natural Science Foundation of China (No. 31970097).

Author contributions

Conceptualization: B.F., Y.L., Y.C., R.B., and D.H. Methodology: Y.L., B.F., R.C., R.B., X.C., D.H., Z.H. and Y.Z. Investigation: Y.L., B.F., R.C., X.C., X.D., J.H., M.C., C.J. Visualization: Y. L., Y.Z. and Y.C. Funding Acquisition: B.F. Project administration: B.F. Writing—Original Draft, B.F., Y.L. and X.W. Writing—Reviewing and Editing: B.F., Y.C., R., Y.L. and Z.H.

Competing interests

The authors declare no competing interests.

Additional information

Supplementary information The online version contains supplementary material available at https://doi.org/10.1038/s41522-024-00586-6.

Correspondence and requests for materials should be addressed to Dejun Hao or Ben Fan.